Photosynthesis Research (2018) 135:285–298
https://doi.org/10.1007/s11120-017-0465-9

ORIGINAL ARTICLE

Mechanisms of drought-induced dissipation of excitation energy in sun- and shade-adapted drought-tolerant mosses studied by fluorescence yield change and global and target analysis of fluorescence decay kinetics

Hisanori Yamakawa[1] · Ivo H. M. van Stokkum[2] · Ulrich Heber[3] · Shigeru Itoh[4]

Received: 27 February 2017 / Accepted: 8 November 2017 / Published online: 18 November 2017

Abstract

Some mosses stay green and survive long even under desiccation. Dissipation mechanisms of excess excitation energy were studied in two drought-tolerant moss species adapted to contrasting niches: shade-adapted *Rhytidiadelphus squarrosus* and sun-adapted *Rhytidium rugosum* in the same family. (1) Under wet conditions, a light-induced nonphotochemical quenching (NPQ) mechanism decreased the yield of photosystem II (PSII) fluorescence in both species. The NPQ extent saturated at a lower illumination intensity in *R. squarrosus*, suggesting a larger PSII antenna size. (2) Desiccation reduced the fluorescence intensities giving significantly lower F_0 levels and shortened the overall fluorescence lifetimes in both *R. squarrosus* and *R. rugosum*, at room temperature. (3) At 77 K, desiccation strongly reduced the PSII fluorescence intensity. This reduction was smaller in *R. squarrosus* than in *R. rugosum*. (4) Global and target analysis indicated two different mechanisms of energy dissipation in PSII under desiccation: the energy dissipation to a desiccation-formed strong fluorescence quencher in the PSII core in sun-adapted *R. rugosum* (type-A quenching) and (5) the moderate energy dissipation in the light-harvesting complex/PSII in shade-adapted *R. squarrosus* (type-B quenching). The two mechanisms are consistent with the different ecological niches of the two mosses.

Keywords Chlorophyll fluorescence · Drought tolerance · Fluorescence lifetime · Photodamage · Moss photosynthesis · Global analysis

The paper is dedicated to Ulrich Heber, who died on June 11, 2016, at the age of 85.

Electronic supplementary material The online version of this article (https://doi.org/10.1007/s11120-017-0465-9) contains supplementary material, which is available to authorized users.

✉ Shigeru Itoh
itoh2nd@gmail.com

[1] Graduate School of Bioagricultural Sciences, Nagoya University, Furocyo, Chikusa, Nagoya 464-8602, Japan

[2] Faculty of Science, Institute for Lasers, Life and Biophotonics, Vrije Universiteit Amsterdam, De Boelelaan 1081, 1081 HV Amsterdam, The Netherlands

[3] Julius von Sachs Institute of Biological Sciences, University of Würzburg, Würzburg, Germany

[4] Division of Material Science (Physics), Graduate School of Science, Nagoya University, Furocyo, Chikusa, Nagoya 464-8602, Japan

Abbreviations

Chl	Chlorophyll
DAS	Decay-associated spectra
F_0 and F_M	Fluorescence yield levels at the dark-adapted and illuminated maximum conditions, respectively
F684, F695, and F730	Fluorescence bands at 684, 695, and 730 nm, respectively
IRF	Instrument response function
LHCII	Light-harvesting complex II
NPQ	Nonphotochemical quenching of fluorescence
PAM	Pulse amplitude-modulated fluorescence measurement
PPFD	Photosynthetic photon flux density
PSI and PSII	Photosystems I and II, respectively

PSIIRC	Reaction center of PSII
red-Chl	Chlorophyll *a* species with long-wavelength fluorescence band
SAS	Species-associated spectra

Introduction

Some mosses survive under sunshine even after full desiccation, keeping their green color. The feature is apparently similar to those reported in many lichens (Heber 2008; Yamakawa et al. 2012; Yamakawa and Itoh 2013), and it is not known yet in higher plants. Although multiple dissipation mechanisms of excess excitation energy are known to be activated by strong illumination to avoid photodamage in hydrated plants (Demmig-Adams 1990; Niyogi 1999), they could not be activated under dehydrated conditions. In the desiccated photosynthetic organisms, the light energy absorbed by the desiccated photosynthetic pigments would kill them because almost all of the physiological or biochemical activities, which are expected to scavenge the radicals, are suppressed. In desiccated lichens, another type of energy dissipation mechanism was shown to be activated (Heber 2008). Studies of the lifetime of chlorophyll fluorescence indicated fast dissipation of excitation energy into heat in photosystem II of dehydrated lichens (Veerman et al. 2007; Komura et al. 2010; Slavov et al. 2013). A recent study indicated the actions of similar mechanisms in some drought-tolerant mosses (Yamakawa et al. 2012, 2013). The drought tolerance in mosses, however, seems to vary significantly depending on the species, seasons, or environmental conditions (Heber 2008; Yamakawa et al. 2012; Yamakawa and Itoh 2013). In this paper, we studied the energy dissipation mechanisms in two moss species that belong to the same family, *Rhytidiaceae*: shade-adapted *Rhytidiadelphus squarrosus* and sun-tolerant *Rhytidium rugosum*. Both are desiccation tolerant but have contrasting light adaptation features. *R. rugosum* was shown to have a drought-induced energy dissipation mechanism similar to that found in many lichens by the analysis of fluorescence lifetime (Yamakawa and Itoh 2013). The different light responses of these mosses may come from different energy dissipation mechanisms although it is not clear yet whether the shade-adapted mosses have the mechanism of efficient energy dissipation.

In hydrated plants, the dissipation of excess excitation energy into heat is known to protect the photosystems from photodamage, as monitored by the decreased fluorescence yield of chlorophyll (Chl) *a* in photosystem II (PS II) (Demmig-Adams 1990; Niyogi 1999; Horton et al. 2005; Papageorgiou 2012). At the start of illumination, the fluorescence yield increases from the low, dark-adapted F_0 level to the high, steady-state F_M level caused by photoreduction of the PSII primary electron acceptor plastoquinone (Q_A). The F_M level, then, is decreased by multiple mechanisms of excess energy dissipation (Demmig-Adams 1990; Niyogi 1999). Typically, the high light-induced electron transfer reaction protonates the intrathylakoid proteins, accumulates xanthophyll/zeaxanthin, and induces the nonphotochemical quenching (NPQ) of fluorescence (Demmig-Adams 1990). This process could be mimicked by the acidification caused by CO_2 in mosses (Yamakawa et al. 2012). Other mechanisms are also known to decrease the excitation energy from PSII, such as the state transition, which seems to occur as a result of the movement of antenna proteins from PSII to PSI, the spillover of excitation energy from PSII to PSI (Murata 1969; Aro et al. 1993; Demmig-Adams 1990; Niyogi 1999; Papageorgiou 2012), or the aggregation of antenna proteins (Horton et al. 2005). These mechanisms decrease the F_M level nearly to the F_0 level. However, the excitation energy that remained at the F_0 level might still be dangerous under desiccated conditions, where most of the light-produced harmful radicals could not be dissipated due to the suppression of the electron transfer reactions and the physiological reactions (Heber 2008).

Some lichens show strong drought tolerance. Lichens, *Parmelia sulcata* (Veerman et al. 2007) and *Physciella melanchla* (Komura et al. 2010), decreased Chl fluorescence below the F_0 level severely upon desiccation and significantly reduced the fluorescence lifetime from 0.4 to 1 ns under wet conditions to around 50 ps under dry conditions (Veerman et al. 2007; Komura et al. 2010; Miyake et al. 2011). The drought-induced quenching rate, therefore, is fast enough to compete against the charge separation rate to avoid the harmful radical formation in dried PSII. It was suggested that the excess energy was transferred to the far-red pigment, which was induced by desiccation, and then dissipated into heat (Komura et al. 2010; Miyake et al. 2011). Interestingly, the quenching ability was lost if symbiont algal cells were isolated and cultured outside lichens (Kosugi et al. 2009), and it was recovered again if a sugar component, arabitol, which was contained in the lichen host fungi, was added during the dehydration. It was, therefore, assumed that quenching occurs through alteration of the environments of PSII pigments in algae (Kosugi et al. 2013), although its relation to the long-term survival of algal cells is not yet clear (Carniell et al. 2015). In another lichen, *P. sulcata*, the decay acceleration was not strong enough to fully interpret the decrease in yield so that the outflow of excitation energy from PSII to PSI (spillover mechanism) was proposed as the major mechanism to dissipate the excitation energy (Slavov et al. 2013).

In contrast to lichens, which are mostly drought tolerant (Heber 2008), moss species include both drought-tolerant and drought-sensitive species. In this report, we studied the drought responses of two closely related species of desiccation-tolerant mosses that show contrasting features:

shade-adapted *R. squarrosus* and sun-adapted *R. rugosum*. *R. rugosum* showed strong phototolerance for all seasons and was shown to accelerate PSII fluorescence decay under desiccated conditions (Yamakawa et al. 2012; Yamakawa and Itoh 2013) like many drought-tolerant lichens. Ordinary NPQ mechanisms also work in the moss under hydrated conditions (Heber et al. 2006; Yamakawa et al. 2012). On the other hand, *R. squarrosus* grows only in the shade and does not tolerate full exposure to sunshine; it exhibits marked variations of sensitivity to photodamage (Heber et al. 2006) and is more phototolerant during the dry summer than in the humid winter. Phototolerance appears to be inducible, because it could be modified under laboratory conditions. In this study, the difference between their photoprotection mechanisms, which seem to contribute to their survival under contrasting ecological niches, was studied by analyzing the effects of dehydration on the yields and lifetimes of chlorophyll fluorescence at 300 and 77 K.

Materials and methods

Collection of samples

The mosses *R. rugosum* and *R. squarrosus* (both belonging to the family *Rhytidiaceae*) were collected from different habitats at a hill approximately 20 km from the city of Würzburg, Bavaria, Germany, where rainfall differs with the season and is, at times, scarce. Exposure to and tolerance of light are different in these mosses. Collected mosses were slowly dried in darkness (or under dim light) at room temperature and stored at − 20 °C until use (field-collected moss). In some cases, collected mosses were hydrated by adding water, dark incubated for 60 h at room temperature, and then slowly desiccated (60-h-dark-adapted moss). Fast air transport of the desiccated moss species facilitated the measurements that were reproducible in both Germany and Japan.

Measurement of fluorescence yield at room temperature

Modulated chlorophyll fluorescence emitted from dry or wet moss thalli at above 700 nm was measured according to Schreiber et al. (1986) with a PAM fluorometer (model 101, Walz, Effeltrich, Germany) after excitation with a 650-nm measuring beam of very low intensity. The strong actinic light pulse and the long actinic illumination were provided by additional halogen lamps (KL 1500, Schott, Mainz, Germany). White light from the lamp was passed through filters (Calflex X and 2× DT Cyan, Balzers, Liechtenstein). Far-red light capable of a specific oxidation of P700 in PSI was obtained through RG 9 (Schott) and Calflex X (Balzers) filters. Dry moss thalli were placed inside the measuring cuvette. Dry thalli in the cuvette were hydrated by adding a small amount of water and then dehydrated again by natural water evaporation. Changes in fluorescence yield during hydration, dehydration, and actinic light illumination of thalli were continuously monitored by the PAM fluorometer.

Measurement of fluorescence lifetime at room and cryogenic temperatures

The absorption spectrum of a single thallus of moss was measured with a homemade spectrometer, in which a fiber light guide from a monochromator (BLK-CXR-SR, StellarNet, Tampa, FL, USA) replaced an eyepiece lens on a microscope (BH-2, Olympus, Tokyo, Japan). The light guide collected the light passed through a small focusing point on the specimen.

Fluorescence lifetimes of mosses were measured as reported (Komura et al. 2006; Komura and Itoh 2009) at weak intensities of excitation laser to enable the measurements under nearly dark-adapted condition. Dark-adapted dry or wet moss thalli were fixed on a sample holder and set in a liquid nitrogen cryostat (N90, Oxford Co., Oxford, UK). The excitation pulse at 430 nm was generated by a thin type I β-barium borate (BBO) crystal from an 860-nm flash of a Ti:Sapphire laser (Mai Tai, Spectra-Physics, Irvine, CA, USA) with a flash duration of 150 fs and a repetition rate of 80 MHz after passing through a 430-nm interference filter to give the intensity at 10 μW at the sample surface in the measurement of *R. rugosum*. In the measurement of *R. squarrosus*, a 405-nm pulse from a laser diode (M4734-32, Hamamatsu Photonics, Hamamatsu, Japan) with the duration of 50 ps at 1.0 μW passed through a 405-nm interference filter was also used for technical reasons at a 1 MHz repetition rate. The two lasers gave similar results within the range of analysis in the present study. The emitted fluorescence was focused onto the entrance slit and diffracted in a 50-cm polychromator as for wavelength, dispersed in a streak camera as for arrival time, and detected with a charge capacitance detector (Chromex 2501-S, 100 g/mm monochromator in Streak Scope C4334, Hamamatsu Photonics, Hamamatsu, Japan). The streak-camera system was operated in the photon-counting mode to give 2-dimensional (2D) images in (640 pixels for wavelength) × (480 pixels for delay time), as shown in Figs. 5 and 6. Each image covered photon counts at 636–778 nm and in the time range of 0–1100 ps (1-ns time base measurement) or 0–5350 ps (5-ns time base measurement). Photon counts were accumulated for approximately 1 h for each image. The images were analyzed with the homemade software as reported previously (Komura et al. 2006, 2010; Yamakawa et al. 2012; Yamakawa and Itoh 2013) to give a fluorescence decay time course at each wavelength or a fluorescence spectrum at each delay time,

which can be calculated as a vertical or horizontal slice of the image. For all room-temperature data, the Full Width at Half Maximum (FWHM) of the Instrument Response Function (IRF) were 21 ps with the 1-ns time base measurements of *R. rugosum* and 144 ps with the laser diode excitation of 50 ps duration (used with *R. squarrosus*). At 77K, the FWHM of the IRF was 17 ps with the 2-ns time base measurements of *R. rugosum* or 151 ps for the measurement of *R. squarrosus*.

Global analysis of fluorescence data

The global analyses of streak images were done with the help of Glotaran that uses the R package TIMP (Mullen and van Stokkum 2007; Snellenburg et al. 2012). A Gaussian shape was assumed for the IRF in the analyses. Target analysis was done as described in Snellenburg et al. (2012).

Results

Field observations

The growth of two closely related moss species, *R. rugosum* and *R. squarrosus*, shown in Fig. 1, was monitored on a hill about 20 km from the city of Würzburg, Bavaria, Germany. The soil and amount of sunshine in their growing places were different: *R. rugosum* grows on fully sun-exposed rocky calcareous soil, while *R. squarrosus* grows on richer, loamy soil shaded by a large willow tree and under a grass cover. During frequent dry periods in the summer, the mosses were dried towards full desiccation with almost no growth. For *R. squarrosus*, the covering by grass and shading by the willow tree were important for survival. Experimental removal of the grass cover accelerated desiccation and initiated a gradual loss of chlorophyll from the moss. Although attempts to revive bleached (chlorophyll-free) thalli by cultivation in a moist atmosphere were not successful in the dark, sprouting of green shoots from bleached thalli was observed under very low light (PPFD at 1.2 µmol m^{-2} s^{-1}; K. Gutekunst, private communication). However, no damage to *R. squarrosus* occurred if the full shade cover was maintained during prolonged desiccation.

Effects of dehydration and rehydration on moss appearance and absorption spectra

Under natural desiccation conditions in the laboratory, the drought-tolerant mosses shrank, showing their thalli overlapping (Fig. 1). However, their appearance and color did not change significantly. Their absorption spectra show typical absorption peaks of Chl *a* at around 677 nm and shoulders at 650 nm. The distinct shoulder band indicates high Chl *b*

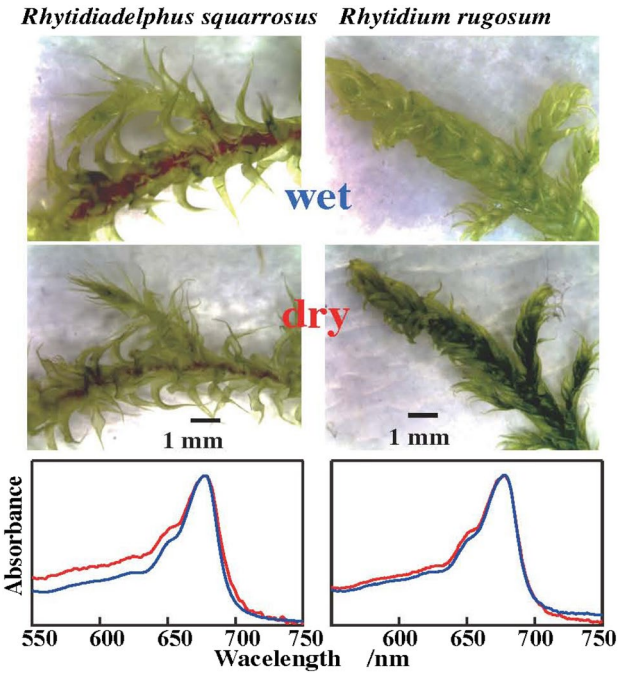

Fig. 1 Images of wet and dry thalli of mosses *Rhytidiadelphus squarrosus* (left) and *Rhytidium rugosum* (right) and their absorption spectra measured at room temperature (bottom). Blue and red lines represent the spectra measured under wet and dry conditions, respectively

content, which is typical for mosses that have a more abundant light-harvesting LHCII complex than higher plants. Desiccation increased light scattering from the surface. However, the absorption spectra, which were normalized at the Chl *a* peaks and corrected for the baseline shifts due to scattering changes, were not modified significantly by desiccation, suggesting only subtle changes of the structure of LHCII or of the aggregation state of Chls in the chlorophyll–protein complexes. The results gave us an opportunity to compare the mechanism of excess energy dissipation in dry *R. rugosum* and *R. squarrosus*.

Effects of desiccation on fluorescence yield

We measured the effects of hydration/dehydration upon the chlorophyll fluorescence yield in the thalli of *R. squarrosus*. The thalli were placed on the sample holder, and the fluorescence yield change upon the addition of distilled water was monitored (Fig. 2). The yields excited by the weak modulation light without and with the preceding strong 1-s actinic flash, which was given every 500 s, were monitored as the F_0 and F_M levels, respectively (Fig. 2). Upon the start of measurement, dried thalli showed a low F_0 level (designated as F_{0d} in Fig. 2). Illumination of strong actinic flashes did not change the yield in this stage. Then, the addition of a small amount of H_2O increased the F_0 level. After the initial fast increase, which seems to be partially due to the change

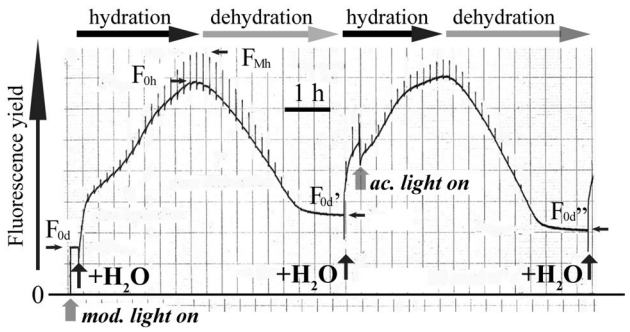

Fig. 2 Effects of slow hydration and dehydration on the time course of the modulated fluorescence intensity of *R. squarrosus*. After the onset of modulating light, the hydration of dry moss thalli increased fluorescence yield gradually from the low initial F_{0d} level to the higher F_{0h} level, and then subsequent slow natural desiccation decreased the fluorescence yield again to the low F_{0d}' level. In the second cycle, desiccated thalli were rehydrated, illuminated with saturating white light at PPFD = 400 μmol m^{-2} s^{-1}, and then slowly desiccated to give the F_{0d}'' level

in light scattering, the F_0 level increased for about 3 h until hydration of the whole thalli. The F_M level, which was at the same level as the F_0 level in the dehydrated state, also increased with hydration. After reaching the maximum (designated as F_{Mh}), the F_0 and F_M levels declined again with the natural dehydration and attained the F_{0d}' level, which was slightly higher than the initial F_{0d} level. The F_{0d}'/F_{0d} ratio was 1.75 in Fig. 2.

During the increase of yield in the second hydration phase, illumination by the strong actinic light at PPFD = 400 μmol m^{-2} s^{-1} decreased the F_V level, giving smaller F_V/F_M ratios. The F_{0d}'' level, which was attained after full dehydration, was then lower than the F_{0d}' level by about 20%, indicating that the F_0 level also decreased after the strong actinic illumination during dehydration. On the other hand, full hydration/dehydration effects could be attained much faster (within 10 min) if the thalli were directly soaked in water or rapidly dried by the blowing of dry air, respectively (not shown), as previously reported (Yamakawa et al. 2012). The results in Fig. 2 were similar to those observed in sun-adapted *R. rugosum* (Yamakawa and Itoh 2013 and see Fig. S1). In *R. rugosum*, the F_0 and F_M levels were strongly quenched upon desiccation, similar to those observed in *R. squarrosus* (Fig. 2), with the larger F_V/F_M ratio (see Fig. S1).

Table 1 summarizes the results of similar experiments in the desiccated thalli of *R. squarrosus* and *R. rugosum*, which were field collected and dark desiccated (condition A) or hydrated and dark incubated for 60 h (condition B) and dark desiccated before the measurements. The suppressing effects of desiccation on F_0 values were represented as the low F_{0d}/F_{0h} ratios of 0.37 and 0.22 in *R. rugosum* and *R. squarrosus*, respectively. The extents of variable fluorescence, represented as the F_V/F_M ratios, were smaller in dry *R. squarrosus* and became larger after the 60-h dark incubation in both species. Illumination during desiccation gave the lower F_0 levels (lower F_{0d}''/F_{0d}' ratios) in both species.

It is concluded that both species show significant desiccation-induced decreases in the F_0 and F_M levels. It is also shown that illumination during desiccation resulted in slightly lower F_0 levels, yielding the F_{0d}''/F_{0d}' ratios of less than 1.0. The desiccation effects, including the effects of illumination during desiccation, were not suppressed by dithiothreitol (DTT) in both species (Table 1), so it is difficult for the drought-induced quenching to be explained by the zeaxanthin-dependent energy dissipation mechanism.

Table 1 Change of fluorescence yield in *R. rugosum* and *R. squarrosus* under different conditions

Condition	F_{0d}/F_{0h} (desiccation effect on F_0)	F_V/F_M (PSII activity under hydrated condition)		F_{0d}''/F_{0d}' (light effect on F_{0d})	
			+ DTT		+ DTT
R. squarrosus					
Dried after field collection	0.22	0.16	0.12	0.82	0.81
Dried after 60-h wet-dark incubation		0.36	0.44	0.69	0.63
R. rugosum					
Dried after field collection	0.37	0.26	0.28	0.78	0.81
Dried after 60-h wet-dark incubation		0.46	0.38	0.76	0.82

Each value is an average of four PAM measurements obtained in experiments analogous to those in Fig. 2. Hydration was done either with or without 5 mM DTT. The F_V/F_M ratio represents the maximum charge separation probability of PSII under saturating light intensity measured in hydrated mosses. F_{0d}'/F_{0d}'' is the ratio of F_0 values measured under desiccated conditions after desiccation in darkness (F_{0d}') and under light (PPFD = 400 μmol m^{-2} s^{-1}) (F_{0d}''). Field-collected moss thalli were slowly dark desiccated (condition a) or desiccated after hydration and dark adaption for 60 h (condition b), either with or without illumination

Actinic light-induced fluorescence quenching under hydrated conditions

Strong actinic illumination decreased the F_M level in the second rehydration cycle of *R. squarrosus* in Fig. 2. Strong illumination is known to activate the NPQ energy dissipation mechanism in plants (Li et al. 2004; Bonente et al. 2010). The decrease, therefore, indicates the action of NPQ energy dissipation also in hydrated *R. squarrosus*.

The effect of actinic intensity was studied further, as shown in Fig. 3. In the hydrated thalli of *R. squarrosus*, which were 60-h-dark-adapted before the measurement, the F_V/F_M ratio sharply decreased to 85% as the actinic PPFDs increased to 200 µmol m^{-2} s^{-1} and then gradually decreased at the higher actinic intensities (Fig. 3, curve a). On the other hand, the F_V/F_M ratio sharply decreased to 48% until PPFDs of 600 µmol m^{-2} s^{-1} in the hydrated thalli of *R. rugosum* (Fig. 3, curve b).

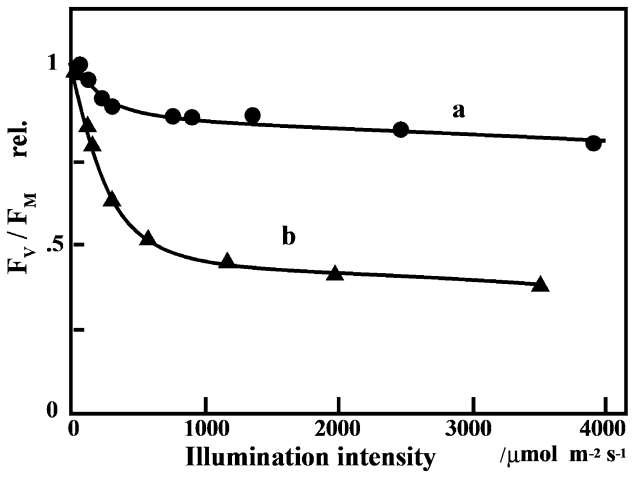

Fig. 3 Effect of the intensity of actinic white light on the F_V/F_M ratio. *a, b* Hydrated thalli of *R. squarrosus* and *R. rugosum*, respectively. The effects of actinic intensities on the steady-state $F_V/F_M = (F_M - F_o)/F_M$ ratios were measured from experiments as in Fig. 2 in two mosses and plotted after normalization. Before the measurements, the mosses were hydrated and dark incubated for 60 h after field collection

The extent of quenching was greater in *R. rugosum* (Fig. 3, curve b) compared to that in *R. squarrosus* (curve a). The effect saturated at the lower actinic intensity in *R. squarrosus*. It suggests that *R. squarrosus* has the larger PSII antenna size compared to that in *R. rugosum*. Therefore, it seems that *R. rugosum*, which shows the stronger quenching ability and smaller antenna, is better adapted to high-light environments than is *R. squarrosus*. However, it is not clear whether these abilities detected under hydrated conditions contribute to energy dissipation under the desiccated condition.

CO_2-induced fluorescence quenching under hydrated conditions

Light-induced activation of NPQ could be mimicked in darkness by adding CO_2 to mosses and lichens (Bukhov et al. 2001; Yamakawa et al. 2012), and dithiothreitol (DTT) inhibited this CO_2 effect in mosses (Yamamoto and Kamite 1972). The CO_2 effect was tested in the hydrated thalli of *R. rugosum* and *R. squarrosus*. Figure 4A shows the effects of incubation with air containing CO_2 on the F_M levels attained after the strong actinic flashes. The addition of CO_2 lowered the F_M levels more significantly than the F_0 levels in *R. squarrosus* (Fig. 4A upper panel). The effect was recovered to 90% after 18 min of flushing with CO_2-free air. A slightly greater extent of CO_2-induced quenching was detected in hydrated *R. rugosum* (Fig. 4A lower panel).

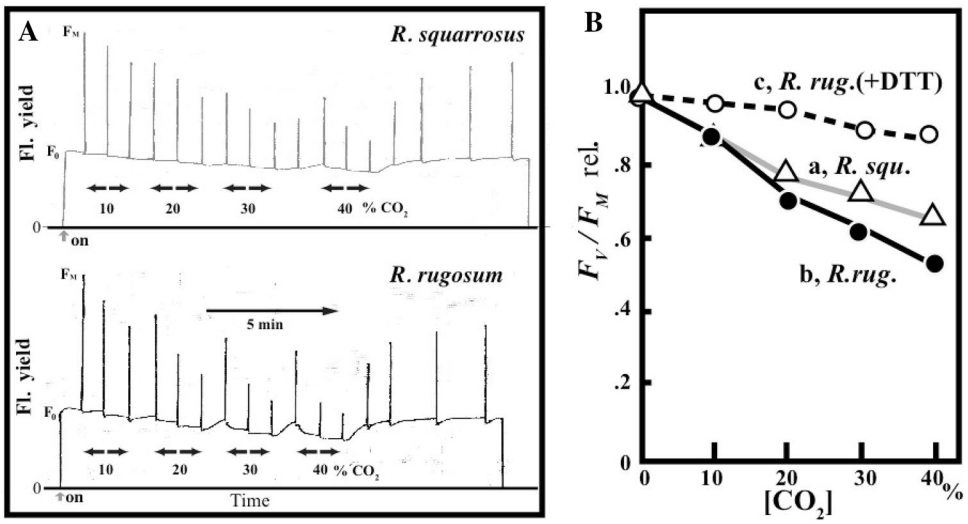

Fig. 4 **A** Effects of CO_2 on the fluorescence yield in hydrated thalli of *R. squarrosus* (upper column) and *R. rugosum* (lower column). Air containing CO_2 was flushed as indicated. **B** Effects of CO_2 concentration on the F_V/F_M ratios in the hydrated thalli of *R. squarrosus* and *R. rugosum*. *a, b R. squarrosus* and *R. rugosum*, respectively. *c R. rugosum* in the presence of 5 mM DTT. $F_V/F_M = (F_M - F_0)/F_M$ ratios were measured as in **A**

Figure 4B shows the evaluation of the effects of CO_2 concentration calculated from the results in Fig. 4A. The F_V/F_M ratios decreased with the increase of CO_2 concentration (curve a) and did so more significantly in *R. rugosum* (curve b). The CO_2 effect was suppressed in the presence of 5 mM DTT in *R. rugosum* (curve c).

The quenching was induced by actinic light or dark CO_2 incubation under the hydrated condition in both moss species. The two types of quenching were almost completely suppressed by DTT, suggesting that they occur as a result of the conversion of xanthophyll/violaxanthin to zeaxanthin. The extent of quenching was greater in sun-adapted *R. rugosum* than in shade-adapted *R. squarrosus*. The difference seems to be related to the different niche selections of the mosses. The drought-induced quenching mechanisms as shown in Fig. 2 were almost insensitive to DTT and did not require illumination. Therefore, the drought-induced strong quenching effect on the F_0 and F_M levels shown in Fig. 2 and Fig. S1 could not be explained by the NPQ mechanism.

Effects of desiccation on fluorescence lifetime and emission spectra at room temperature

Fluorescence decay kinetics was measured in order to further study the mechanism of the desiccation-induced fluorescence quenching. Figure 5 shows the traces of photons emitted in a wavelength range of 680–760 nm (abscissa) and a delay time range of −0.6 to 4.0 ns with respect to the peak time of the excitation laser (ordinate). The wavelength–time 2D images were measured with a streak-camera system as described in "Materials and methods". The image gives either a time-resolved spectrum or a decay time course if integrated for a selected range along the vertical time axis or the horizontal wavelength axis, respectively.

In hydrated *R. squarrosus*, a strong peak of PSII fluorescence was detected at 685 nm at 0 ns just after the time of excitation with the 430-nm laser flash with a 150 fs duration (Fig. 5a). The fluorescence region extended horizontally from the 680-nm peak to the 700–770 nm shoulder region (Fig. 5a). The shoulder is contributed mainly by the PSII shoulder band and partly by the PSI bands. Along the vertical time axis, the 685-nm peak expanded toward the time range longer than 1 ns, indicating the rather long lifetime of the PSII band as reported for other mosses (Yamakawa et al. 2012; Yamakawa and Itoh 2013). In desiccated thalli, the 685-nm band became less marked and gave a shorter vertical expansion indicating a shorter PSII lifetime (Fig. 5b).

In hydrated *R. rugosum*, the image was similar to that of hydrated *R. squarrosus* with more marked vertical elongation indicating a longer lifetime (Fig. 5c). Desiccation shortened the vertical distribution of the 685-nm band (Fig. 5d), indicating a very short lifetime as reported previously (Yamakawa et al. 2012; Yamakawa and Itoh 2013).

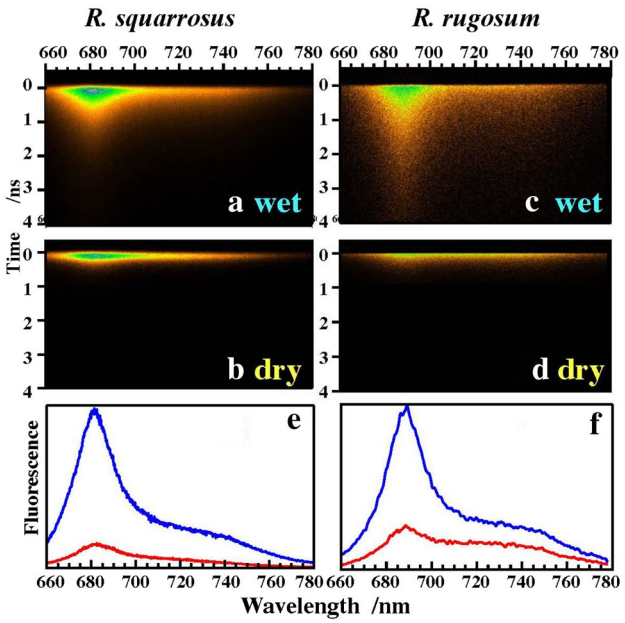

Fig. 5 Effects of desiccation on the wavelength/time 2D fluorescence images (**a**–**d**) and on the emission spectra (**e, f**) of two moss species at room temperature. **a, b** Fluorescence wavelength/time 2D images in wet and dry thalli of *R. squarrosus*, respectively. **c, d** Wet and dry *R. rugosum*. **e, f** Fluorescence emission spectra, which correspond to the steady-state spectra, calculated as the integration of intensities at 0–4 ns after the laser excitation in the above images. Red and blue lines indicate the spectra of wet and dry thalli, respectively. The integrated spectra correspond to the ones measured under continuous excitation light

The fluorescence emission spectra, which correspond to the emission spectra measured by the fluorescence spectrometer under continuous excitation light, were calculated by integrating the emission intensities for the time range of 0–4 ns at each wavelength in the images in Fig. 5a–d. The obtained spectra (Fig. 5e, f) showed peaks at around 685 nm. The intensities were significantly decreased by desiccation in both species (red curves). The result is consistent with the drought-induced suppression of the steady-state PSII fluorescence measured by PAM in Fig. 2. The integrated spectrum of dry *R. squarrosus* (red line in Fig. 5e) showed very low intensities at both the peak and the shoulder when compared to that of the wet one (blue line), while dry *R. rugosum* (red line in Fig. 5f) gave a larger shoulder band, suggesting that the decrease was more specific for PSII, or that a more red-emitting species contributes.

Effects of desiccation on fluorescence decay kinetics at 77 K

Fluorescence kinetics was also measured at 77 K. At this temperature, excitations can be trapped by Chl species that emit at lower energy than the RC pigments. This results in

red-shifted emission with long lifetimes (Fig. 6). On cooling to 77 K, the broad peaks of the PSI fluorescence band at 730 nm (F730) became stronger, with very long-lived vertical tails in the hydrated thalli of both species (Fig. 6a, c). PSII peaks are seen at 684 (F684) and 695 nm (F695). The spectra are very similar to those reported in mosses (Yamakawa et al. 2012; Yamakawa and Itoh 2013). F684 and F695 are known to be emitted from Chls on the CP43 and CP47 subunits of the PSII reaction center complex, respectively, and F730 from the longer wavelength forms of Chl *a*, the so-called "red-Chl" on PSI (de Groot et al. 1999; Komura and Itoh 2009).

The intensities and lifetimes of F730 bands were not affected much by desiccation (Fig. 6b, d). The PSII bands in *R. squarrosus* showed lower intensity but suggested similar lifetimes (Fig. 6b), while those in *R. rugosum* indicated faster decay with significantly shortened tail length along time axis (Fig. 6d), as discussed further below. In the desiccated thalli of *R. squarrosus* and *R. rugosum*, PSII band intensities were suppressed significantly, as observed in the 0–4 ns integrated spectra (red curves in Fig. 6e, f). Under desiccated conditions, both species showed smaller PSII bands and an almost unchanged F730 bands in the integrated spectra, which were slightly blue-shifted in *R. rugosum* (Yamakawa and Itoh 2013). For quantification of these qualitative observations, we globally analyzed the data.

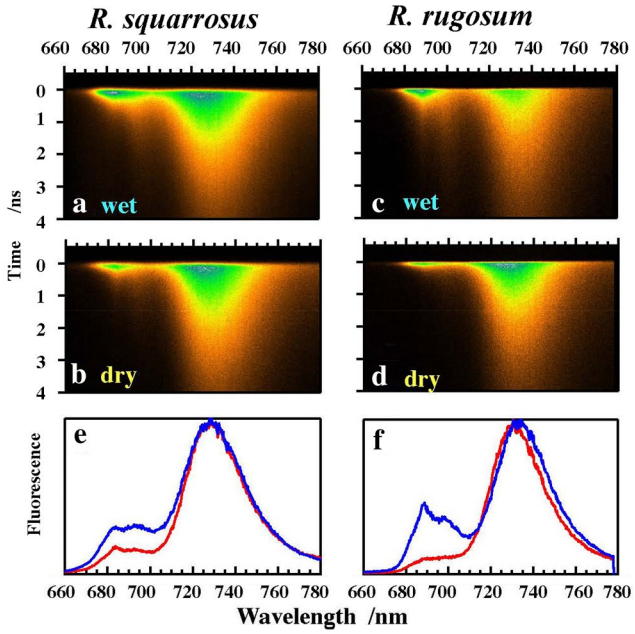

Fig. 6 Effects of desiccation on wavelength/time 2D fluorescence images and emission spectra of two moss species at 77 K. **a, b** Fluorescence wavelength/time images in wet and dry thalli of *R. squarrosus*, respectively. **c, d** Wet and dry *R. rugosum*. **e, f** Integrated fluorescence emission spectra, which correspond to the steady-state spectra, calculated as the 0–4-ns integration of intensities from the above images. Red and blue lines indicate the spectra of wet and dry thalli, respectively

Global analysis of room-temperature fluorescence kinetics: decay-associated spectra (DAS)

Global analysis of fluorescence decay kinetics was done to further investigate the mechanism of fluorescence quenching. Decay-associated spectra (DAS) were estimated from the fluorescence images at room temperature shown in Fig. 5. Negative and positive bands in DAS correspond to decay and rise of excitation energy in the corresponding band, respectively, and give information about the transfer and quenching of excitation energy.

In wet conditions, three lifetimes are needed to globally fit the data of both organisms (Fig. 7a, c; Table 2). It is striking that all DAS are nonnegative, i.e., there are no rise components, indicating that only a small amount of spectral evolution is present. The equilibration process between LHCII and PSII is not visible probably because of the nonselective excitation condition at 430 or 405 nm. Additional measurements with more selective excitation of Chl b would be needed to resolve this equilibration. The first DAS (lifetime 96 or 66 ps in *R. squarrosus* and *R. rugosum*, respectively) is dominated by trapping in PSI. The shapes of the second and third DAS are very similar and can be interpreted as biexponential decay of emission from PSII plus LHCII, with lifetimes of $\approx$0.4 and $\approx$1.4 ns. These lifetimes are rather long and suggest that most of the PSIIRC are in the closed state.

In dry conditions, the two species behave very differently. Fitting of *R. squarrosus* data (Fig. 7b) still requires three lifetimes. The first DAS (lifetime 33 ps) appears to be a mixture of quenching from PSII plus LHCII and trapping in PSI. The spectral shape of the second DAS (red, 0.12 ns) is very similar to the shapes of the red and blue DAS in Fig. 7a. The short lifetime DAS of 0.12 ns indicates that it represents the quenched PSII plus LHCII. The very small 0.63 ns DAS (blue) seems to represent a small amount of mildly quenched PSII plus LHCII. Fluorescence of dry *R. rugosum* (Fig. 8d) can be described by only two lifetimes. The first DAS (lifetime 100 ps, black) is dominated by trapping in PSI. The shape of the second DAS (red, 0.29 ns) in Fig. 7d is different from the shapes of the red and blue DAS in Fig. 7b, with a pronounced shoulder near 740 nm. It suggests that the equilibrium of PSII plus LHCII with a quenched species at 740 nm is present.

Target analysis of room-temperature fluorescence kinetics

Inspired by these observations, a simultaneous target analysis of the measurements in the wet and dry states of *R. rugosum* has been attempted. Under the assumption that the species-associated spectra (SAS) are the same for the wet

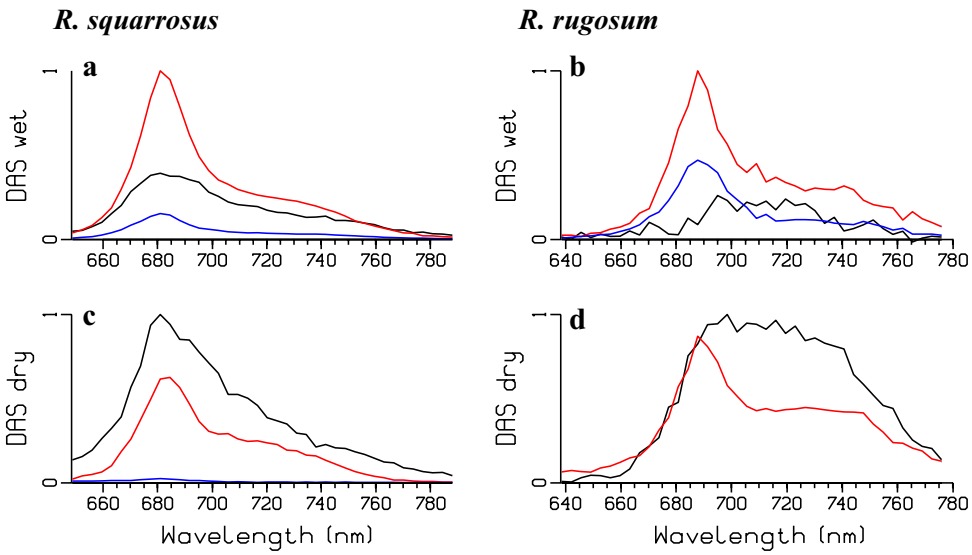

Fig. 7 Estimated DAS of mosses in wet (**a, b**) or dry (**c, d**) condition at room temperature. For lifetimes and color key, see Table 2

Table 2 Estimated lifetimes (in ns) and color key of DAS at room temperature depicted in Fig. 7

Sample	*R. squarrosus*		*R. rugosum*	
Condition	Wet	Dry	Wet	Dry
τ1 (black)	0.096	0.033	0.066	0.100
τ2 (red)	0.43	0.12	0.37	0.29
τ3 (blue)	1.32	0.63	1.45	

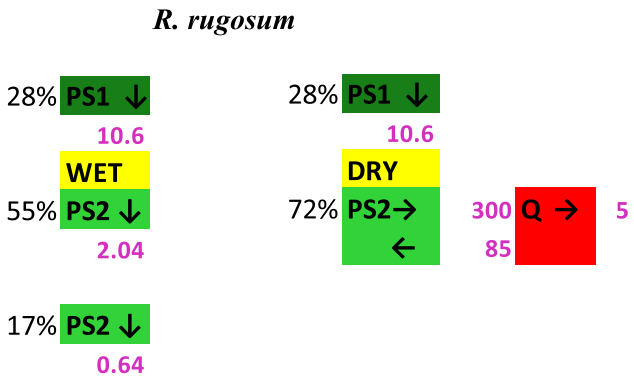

Fig. 8 Target analysis of fluorescence kinetics of *R. rugosum* at room temperature. Functional compartmental model in the wet (left) and dry (right) states. Color key for the three different species: PSI (dark green), PSII plus LHCII (light green), and a quenched species Q (red). All microscopic rate constants are in 1/ns. Percentages to the left indicate the relative excitation

and the dry states, a new SAS for a quenched state can be resolved from the differences between the DAS of the wet and dry states (Fig. 7b, d). Crucial for this assumption is that possible self-absorption does not cause significant differences between the SAS of the wet and dry states. The fact that the absorption spectra were not modified significantly by desiccation (cf. Fig. 1) supports the assumption. The kinetic scheme is depicted in Fig. 8. Since there was no evidence for spillover, we employ independent compartments for PSI (28%, dark green) and PSII plus LHCII (72%, light green). These fractions can be estimated under the assumption that the area under the SAS is equal (Snellenburg et al. 2012). The PSI emission is trapped with a rate of ≈ 11/ns. The biexponential decay of PSII plus LHCII is described by two fractions with decay rates of 2.04/ns (55%) and 0.64/ns (17%) with the measurement with a time base of 1 ns. With the data measured on the time base of 5 ns, these fractions are estimated to be 2.04/ns (37%) and 0.64/ns (35%). This difference is attributed to a larger fraction of PSIIRC in the closed state in the latter. An alternative description for the biexponential decay of PSII plus LHCII fraction would be equilibrium with a nonradiative radical pair state (Slavov et al. 2013). Establishing the best model for the biexponential decay of PSII plus LHCII requires further controlled experiments with a better signal-to-noise ratio.

Assuming that there is no state transition after the desiccation the relative excitation of PSI (28%) remains the same in the dry state. To describe the acceleration of the decay of the PSII plus LHCII emission, a very fast equilibrium with a quenched species Q (red) is needed. This equilibration time of ≈ 3 ps is much shorter than the FWHM of the IRF (21 ps) and thus cannot be estimated. In turn, the quenched species Q decays with a rate of 5/ns. The fit quality of this simultaneous target analysis is excellent, cf. Fig. S3.

The estimated species-associated spectra (SAS) depicted in Fig. 9b are consistent with the properties of the species. PSII plus LHCII (light green) peaks at ≈ 686 nm with a vibrational tail that extends until 780 nm. PSI (dark green) emits more to the red and has a stronger contribution near 720 nm, which we attribute to red-shifted Chl *a* in the core and the peripheral antenna of PS I. The quenched species

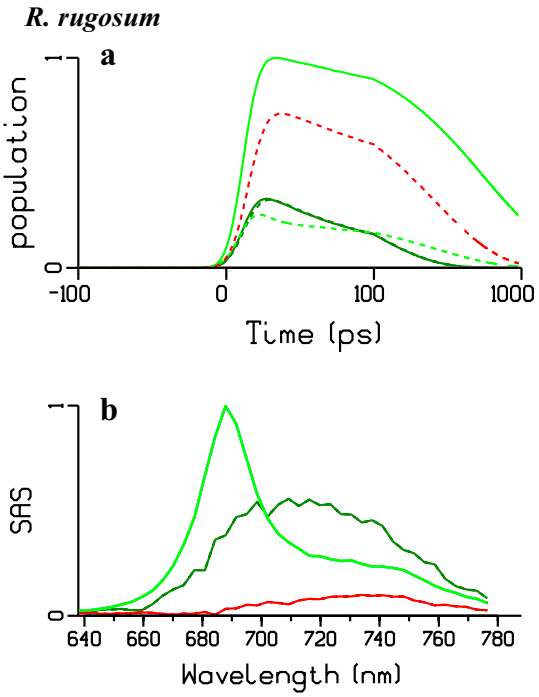

Fig. 9 Target analysis of fluorescence data of *R. rugosum* at room temperature. Estimated total concentrations (**a**) and SAS (**b**). Color key for the three different species: PSI (dark green), PSII plus LHCII (light green), and a quenched species Q (red). Solid and dashed lines in **a** represent the wet and dry states, respectively. Note that the time axis in **a** is linear until 100 ps and logarithmic thereafter

Q (red) has a small oscillator strength (the area under the red SAS is much smaller), with a maximum emission at ≈740 nm.

A simultaneous target analysis of the measurements in the wet and dry states of *R. squarrosus* has been attempted as well. A kinetic scheme that is very similar to that of *R. rugosum* is depicted in Fig. S7. To describe the acceleration of the decay of the PSII plus LHCII emission, a very fast equilibrium with a quenched species Q (red) has been used. This equilibration time of ≈17 ps is much shorter than the FWHM of the IRF (143 ps) of the measurement and thus cannot be estimated. In turn, the quenched species Q decays with a rate of ≈50/ns. The fit quality of this simultaneous target analysis is excellent, cf. Fig. S4. The estimated SAS depicted in Fig. S8B are consistent with the properties of the species, although they are different from the SAS of *R. rugosum* in Fig. 9b. The SAS of PSI (dark green) shows more red-shifted emission than that of PSII plus LHCII (light green). The quenched species Q (red) has a small oscillator strength (the area under the red SAS is much smaller), with a maximum emission at ≈700 nm. However, in view of the short lifetime (≈25 ps) of this Q relative to the FWHM of the IRF (143 ps), this Q species is less well resolved than that of *R. rugosum* in Fig. 9b. Note that about 11% of

Table 3 Estimated lifetimes (in ns) and color key of DAS at 77 K depicted in Fig. 10

Sample	*R. squarrosus*		*R. rugosum*	
Condition	Wet	Dry	Wet	Dry
τ1 (black)	0.020	0.020	0.016	0.009
τ2 (red)	0.117	0.087	0.068	0.045
τ3 (blue)	0.34	0.30	0.27	0.19
τ4 (green)	1.16	1.07	0.87	0.90
τ5 (magenta)	2.15	1.91	2.26	1.99

the excitations (possessing a PSII plus LHCII SAS) decay with a lifetime of 1220 ps or 210 ps in the wet or dry state, respectively. Thus these states are mildly quenched. Such mildly quenched states were not found in *R. rugosum*. The *R. squarrosus* SAS of PSI (dark green) in Figure S 8B possess more emission near 680 nm than the *R. rugosum* SAS of PSI in Fig. 9b. Therefore, with *R. squarrosus* an alternative kinetic scheme was tested, without a quenched species. Instead, spillover in the dried state was allowed for (Fig. S9). The rate of spillover could not be estimated and was fixed at 20/ns. The observed quenching could only be described when the relative input to PSI and PSII plus LHCII was additionally allowed to vary. Thus, the direct input to PSI increased from 33 to 63%. The SAS in the wet and dry states were allowed to differ. The PSII plus LHCII SAS was not significantly different in the dry and wet states (compare orange and light green colors in Fig. S10B). The PSI SAS in the dry state possessed more emission near 680 nm than in the wet state (compare red and dark green colors in Fig. S10B). These observations are consistent with a state transition where during dehydration part of the LHCII antenna detaches from PSII and attaches to PSI, thus increasing the relative input to PSI and the contribution of the 680-nm emission to the PSI (plus LHCII) SAS.

Global analysis of 77K fluorescence kinetics

In all conditions, five lifetimes are needed to globally fit the data at 77K (Table 3). Figure S5 demonstrates the excellent quality of the fit with *R. rugosum*. Four experiments (wet or dry, on a time base of 2 or 5 ns) have been simultaneously analyzed. The FWHM of the IRF was ≈17 or ≈70 ps with a measurement of 2 or 5 ns time base, respectively. From the data with the highest time resolution, rise components of 16 or 9 ps (black DAS in Fig. 10b, d) were estimated in the wet or dry state, respectively. These fast DAS are not conservative, which suggests that after the 430-nm light excited the Soret states the energy transfer to the red-emitting states takes ≈10 ps. It cannot be concluded whether these red-emitting states all belong to PSI or not. Small negative amplitudes are also present with the green DAS (≈900 ps),

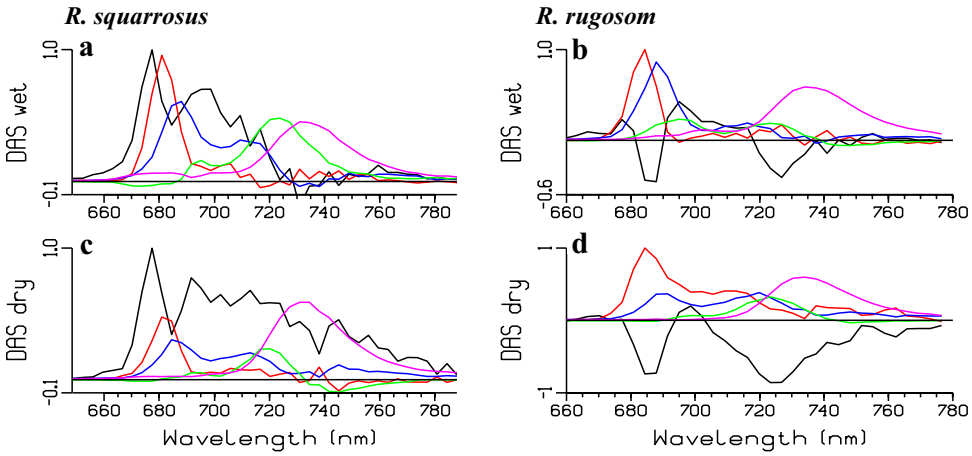

Fig. 10 Estimated DAS of mosses (indicated in the top labels) at 77 K in wet (**a, b**) or dry (**c, d**) condition. See Table 3 for lifetimes and color key

which was also not conservative. The faster decay of the emission in the dry state is visible most clearly in the red and blue DAS. In the PSII region (below ≈710 nm), the ≈900 ps decay (green DAS) and ≈2 ns decay (magenta DAS) are much smaller in the dry than in the wet state. Increases in the red and blue DAS are present in the 700–735 nm region. The negative amplitude in the black DAS in the 705–720 nm region (Fig. 10d) suggests that a quenching species is populated in 9 ps, which decays with ≈45 or ≈190 ps.

With *R squarrosus*, the FWHM of the IRF was ≈120 or ≈145 ps with a measurement time base of 2 or 5 ns, respectively. Therefore, the fastest lifetime cannot be estimated precisely in the measurements. It was fixed at 20 ps and its DAS (black in Fig. 10a, c) was not conservative and showed a small rise component in the 730–745 nm region only (black in Fig. 10a). Small negative amplitudes are also present with the green DAS (≈900 ps), which was not conservative. In the PSII region (below ≈705 nm), the ≈1100 ps decay (green DAS) and ≈2 ns decay (magenta DAS) are again smaller in the dry than in the wet state. Fig. S6 demonstrates the excellent quality of the fit with *R. squarrosus*.

A target analysis of these 77 K data is a subject of further research.

Discussion

Excess excitation energy dissipation in hydrated mosses

Two species of mosses that are drought tolerant and phylogenetically close to each other should have energy dissipation mechanisms to avoid photodamage under both hydrated and dehydrated conditions. Under hydrated conditions, both species showed NPQ. The sun-adapted *R. rugosum* showed stronger quenching that saturated at a larger illumination intensity. The feature of the NPQ mechanism in the moss is similar to that known in hydrated higher plants and explains the adaptation to strong sunshine (Fig. 4). Hydrated thalli of *R. squarrosus* exhibited a similar light-induced energy dissipation mechanism. However, the extent of quenching was lower. It saturated at weaker actinic light intensities, suggesting a larger antenna size, as expected for shade-adapted plants. A weak acid (dissolved CO_2), which supports the protonation-type energy dissipation mechanism in mosses (Yamakawa et al. 2012), decreased the fluorescence yields in both species (Fig. 2). DTT suppressed the CO_2-induced quenching. Therefore, the two moss species have light-induced fluorescence quenching abilities under hydrated conditions similar to those observed in ordinary green plants (Aro et al. 1993; Demmig-Adams 1990; Niyogi 1999; Li et al. 2004; Papageorgiou 2012). The greater extent of quenching that saturated at the higher actinic intensity suggests a smaller antenna size in the sun-adapted *R. rugosum*. Therefore, the energy dissipation behaviors of the two hydrated moss species explain their sun-adapted and shade-adapted natures well. However, under desiccated conditions, actinic illumination no more changed the fluorescence yield in the two mosses (Fig. 2). Therefore, mechanisms, which are different from the light-induced NPQ, are needed to explain the strong desiccation-induced quenching which are insensitive to DTT in both moss species.

Fluorescence yield under desiccated conditions

Dehydration decreased the F_0 levels to 0.22 and 0.37 in *R. squarrosus* and *R. rugosum* (Fig. 2; Table 1), respectively. This is in contrast to the situation in ordinary plants, such as spinach, that show no significant F_0 quenching or decay acceleration by desiccation (see Fig. S2). It was also shown in the present study that the decreased fluorescence yields in dry mosses no longer responded to actinic illumination. On the other hand, illumination during desiccation slightly affected the F_{0d} level attained after desiccation, suggesting

some relation between the desiccation-induced quenching and the light-induced quenching. However, DTT, which is an inhibitor of NPQ, eliminated neither the desiccation-induced quenching nor the light effect on it (Fig. 2; Table 1). Therefore, energy dissipations under the dehydrated condition are suggested to come from a mechanism different from the NPQ mechanism that occurs only under the hydrated condition.

The higher F_{0d}/F_{0h} ratio in *R. rugosum* in Table 1 apparently suggests the desiccation-induced quenching weaker than that in *R. squarrosus*. However, it rather contradicts the conclusion from the lifetime analysis in Figs. 5, 6, and 7 that indicated the stronger PSII quenching in *R. rugosum*. The apparent contradiction seems to be explained by the higher contribution of PSI fluorescence to F_{0d} detected by the present PAM measurement, which detects all the emissions above 700 nm. The integrated fluorescence spectrum of desiccated *R. rugosum* in Fig. 5f shows the higher shoulder band above 700 nm. It explains the detected higher F_{0d} level even with the stronger PSII quenching in this species. Therefore, careful spectral and kinetic analyses as done in this study are important to know the mechanism of severe quenching of the F_0 level induced by dehydration.

Desiccation-induced fluorescence lifetime changes in sun-adapted *R. rugosum*: type-A quenching

Fluorescence decay/yield of PSII, but not PSI, was significantly affected by desiccation in *R. rugosum*, both at room temperature and at 77 K (Figs. 5, 6). The strong decay accelerations interpret the decreased fluorescence yield. As summarized in target analysis of fluorescence lifetime measurements at room temperature in Fig. 8, it can be assumed that almost all the excitation energy on PSII is transferred to a desiccation-induced quencher, which weakly emits at around 740 nm, very rapidly. This mechanism, designated as type-A quenching in this paper, resembles that reported in other desiccation-tolerant moss species (Yamakawa et al. 2012; Yamakawa and Itoh 2013) or desiccation-tolerant lichens (Komura et al. 2010; Miyake et al. 2011). It has been proposed that either a long-wavelength form of chlorophyll *a* or its oxidized form may work as the quencher to accumulate the excitation energy to be dissipated into heat. This idea has explained the fluorescence decay accelerations at 77 K (Veerman et al. 2007; Komura et al. 2010) and at 5 K (Miyake et al. 2011) for lichens, as well as for the desiccation-tolerant mosses *C. purpureus* and *R. rugosum* at 77 K (Yamakawa et al. 2012; Yamakawa and Itoh 2013). Therefore, we assume that the type-A quenching mechanism decreased the fluorescence yield (integrated intensity) significantly in *R. rugosum* at both room temperature and 77 K. At room temperature, in our target analysis we found that PSII plus LHCII quickly (in ≈3 ps) equilibrate with a quencher that has a small oscillator strength, emits near 740 nm, and decays with a rate of 5/ns (Figs. 8, 9). This SAS (Fig. 9) resembles the SAS of a charge transfer (CT) state resolved by Slavov et al. (2013) in a target analysis of desiccation-induced excited state quenching in *Parmelia* lichen.

Desiccation-induced fluorescence lifetime change in shade-adapted *R. squarrosus*: type-B quenching

The desiccation-induced quenching in *R. squarrosus* also significantly shortened the decay time constant at room temperature but less at 77 K. The target analysis of the room-temperature measurements is less reliable because of the much wider IRF (FWHM 143 ps) of this measurement. Nevertheless, a first target analysis, where the acceleration of the decay of the PSII plus LHCII emission is described by a very fast equilibrium with a quenched species Q (Figs. S7 and S8), indicates that (57/68 =) 84% of the PSII plus LHCII equilibrate with a quencher that has a small oscillator strength, emits near 710 nm, and decays with a rate of 49/ns. The remaining (11/68=) 16% of the PSII plus LHCII are only mildly quenched with a rate of 4.8/ns, showing no evidence for the involvement of a quencher. In an alternative target analysis of *R squarrosus* at room temperature, the acceleration of the decay of the PSII plus LHCII emission can be described by spillover to PSI, in combination with a state transition. Similar to the first target analysis, (7/37 =) 18% of the PSII plus LHCII are only mildly quenched with a rate of 2.7/ns (Fig. S9). A target analysis of the 77 K data in future could probably help decide between these two different kinetic schemes. Although we do not yet know the mechanism, we observe that the quenching in *R. squarrosus* does not fully accelerate the PSII decay. We tentatively denote it as type-B quenching. In this proposed type-B quenching, a small amount (16 or 18%) of slowly decaying PSII plus LHCII emission remains even in the dry state. At 77 K, the quenching of PSII plus LHCII was larger in *R. rugosum* than in *R. squarrosus* (compare panels e and f of Fig. 6, and also the DAS in Fig. 10). Whether the quenching in *R. squarrosus* is only quantitatively different from that in *R. rugosum*, or qualitatively, will have to await a target analysis of the 77-K data.

The B-type quenching process, therefore, resembles the "state shift" or "spillover" mechanisms, which were proposed to work to decrease the apparent size of PSII antenna. However, they work only under hydrated conditions. The "state shift" is proposed to occur via the movements of antenna complexes from PSII to PSI, and the "spillover" via the increase of energy transfer from PSII antenna pigments to PSI (Murata 1969; Schreiber et al. 1986; Niyogi 1999; Papageorgiou 2012). As for the desiccation-induced fluorescence quenching at room temperature of a lichen *P. sulcata*, Slavov et al. (2013) proposed that the major portion

of excitation energy in PSII is decreased by the spillover to PSI based on the target analysis of fluorescence decay kinetics at room temperature.

Final remarks

It seems natural that the quenching mechanisms are different between the shade-adapted *R. squarrosus* and the sun-adapted *R. rugosum*. The latter situation seems to be similar for another sun-adapted drought-tolerant moss, *C. purpureus* (Yamakawa et al. 2012; Yamakawa and Itoh 2013).

We assume that the two type-A or -B energy dissipation mechanisms are induced to dissipate the excess excitation energy from PSII by the desiccation in drought-tolerant mosses. The type-A quenching accompanies the significant decay acceleration due to the desiccation-induced quencher inside the PSII core. This type is also seen in sun-adapted *R. rugosum, C. purpureus*, or symbiont green algae inside the lichen *P. melanchla* (Komura et al. 2010; Yamakawa et al. 2012; Yamakawa and Itoh 2013). On the other hand, the type-B quenching mechanism, shown in *R. squarrosus*, also seems to work to decrease the excitation energy from PSII probably situated in LHC or PSII peripheral. However, even with the action of the type-B mechanism, some excitons that have attained the PSII core Chls could not fully be dissipated, especially at a low temperature, as seen from the apparently unaffected PSII fluorescence lifetime at 77 K. Therefore, type-B mechanism, which protects the dehydrated PSII from photodamage under moderate light, may not be sufficient to fully cut the damage under strong sunshine because even a small amount of excitation energy will damage the dry PSII, in which electron transfer has stopped. The contribution of type-B quenching to the survival of *R. squarrosus* remains to be tested.

The molecular mechanisms of the drought-induced type-A and type-B quenching mechanisms are not yet clear. We could assume type-B to occur by modifications of the arrangements of antenna Chls in analogy to the light-induced quenching mechanisms induced by aggregation or modification of light-harvesting proteins (Aro et al. 1993; Demmig-Adams 1990; Niyogi 1999; Horton et al. 2005; Li et al. 2004). Type-A may occur by another mechanism. However, It seems that the type-A and type-B quenching mechanisms are somewhat different from the light-induced quenching mechanisms like NPQ that operate only under hydrated conditions. It seems also probable that type-A and type-B quenching mechanisms co-operate in one organism. No similar drought-induced quenching mechanisms have been found in higher plants. It is clear that the occupation of widely different habitats by mosses is accomplished by the regulatory usage of multiple energy dissipation mechanisms under both wet and dry conditions.

Acknowledgements This work was financially supported by the Ministry of Education, Culture, Sports, Science, and Technology (KAKENHI Nos. 26440139 and 17K07440) to S.I. The authors thank Dr. Yoshimasa Fukusima at Advanced Research Institute for Natural Science and Technology in Osaka City University for his help in DAS analysis. H. M. and S. I. thank Dr. Masahiro Ishiura at the Center for Gene Research and Tsutomu Kouyama at the Department of Physics in Nagoya University for their encouragement during the work.

References

Aro EM, Virgin I, Andersson B (1993) Photoinhibition of photosystem II. Inactivation, protein damage and turnover. Biochem Biophys Acta 1143:113–134

Bonente G, Ballotari M, Truong TB, Morosinotto T, Ahn TK, Fleming GR, Niyogi KK, Bassi R (2010) Analysis of LhcSR3, a protein essential for feedback de-excitation in the green alga *Chlamydomonas reinhardtii*. PLoS Biol 9, e1000577

Bukhov NG, Kopecky J, Pfündel EE, Klughammer C, Heber U (2001) A few molecules of zeaxanthin per reaction centre of photosystem II permits effective thermal dissipation of light energy in a poikilohydric moss. Planta 212:739–748

Carniell FC, Zanelli D, Bertuzzi S, Tretiach M (2015) Desiccation tolerance and lichenization: a case study with the aeroterrestrial microalga *Trebouxia* sp. (*Chlorophyta*). Planta 242:493–505

Demmig-Adams B (1990) Carotenoids and photoprotection of plants: a role for the xanthophyll zeaxanthin. Biochem Biophys Acta 1020:1–24

Groot ML, Frese RN, de Weerd FL, Bromek K, Pettersson A, Peterman EJ, van Stokkum IHM, van Grondelle R, Dekker JP (1999) Spectroscopic properties of the CP43 core antenna protein of photosystem II. Biophys J 77:3328–3340

Heber U (2008) Photoprotection of green plants: a mechanism of ultra-fast thermal energy dissipation in desiccated lichens. Planta 228:641–650

Heber U, Bilger W, Shuvalov VA (2006) Thermal energy dissipation in reaction centres and in the antenna of photosystem II protects desiccated poikilohydric mosses against photooxidation. J Exp Bot 57:2993–3006

Horton P, Wentworth M, Ruban A (2005) Control of the light harvesting function of chloroplast membranes: the LHCII-aggregation model for non-photochemical quenching. FEBS Lett 579:4201–4206

Komura M, Itoh S (2009) Fluorescence measurement by a streak camera in a single-photon-counting mode. Photosynth Res 101:119–133

Komura M, Shibata Y, Itoh S (2006) A new fluorescence band F689 in photosystem II revealed by picosecond analysis at 4–77 K: function of two terminal energy sinks F689 and F695 in PS II. Biochem Biophys Acta 1757, 1657–1668

Komura M, Yamagishi A, Shibata Y, Iwasaki I, Itoh S (2010) Mechanism of strong quenching of photosystem II chlorophyll fluorescence under drought stress in a lichen, *Physciella melanchla*, studied by subpicosecond fluorescence spectroscopy. Biochem Biophys Acta 1797:331–338

Kosugi M, Arita M, Shizuma R (2009) Responses to desiccation stress in lichens are different from those in their photobionts. Plant Cell Physiol 50:879–888

Kosugi M, Miyake H, Yamakawa H, Shibata Y, Miyazawa A, Sugimura T, Satoh K, Itoh S, Kashino Y (2013) Arabitol provided by lichenous fungi enhances ability to dissipate excess light energy in a symbiotic green alga under desiccation. Plant Cell Physiol 54:1316–1325

Li X-P, Gilmore AM, Caffari S, Bassi R, Golan T, Kramer D, Niyogi KK (2004) Regulation of photosynthetic light harvesting involves intrathylakoid lumen pH sensing by the PsbS protein. J Biol Chem 279:22866–22874

Miyake H, Komura M, Itoh S, Kosugi M, Kashino Y, Satoh K, Shibata Y (2011) Multiple dissipation components of excess light energy in dry lichen revealed by ultrafast fluorescence study at 5 K. Photosynth Res 110:39–48

Mullen KM, van Stokkum IHM (2007) TIMP: an R package for modeling multi-way spectroscopic measurements. J Stat Softw 18(3):1–46

Murata N (1969) Control of excitation transfer in photosynthesis. Light-induced change of chlorophyll *a* fluorescence in *Porphyridium cruentum*. Biochem Biophys Acta 172:242–251

Niyogi KK (1999) Photoprotection revisited: genetic and molecular approaches. Annu Rev Plant Physiol Plant Mol Biol 50:333–359

Papageorgiou GC (2012) Fluorescence emission from the photosynthetic apparatus. Adv Photosynth Respir 34:415–443

Schreiber U, Schliwa U, Bilger W (1986) Continuous recording of photochemical and non-photochemical chlorophyll fluorescence quenching with a new type of modulation fluorometer. Photosynth Res 10:51–62

Slavov C, Reus M, Holzwarth AR (2013) Two different mechanisms cooperate in the desiccation-induced excited state quenching in *Parmelia* lichen. J Phys Chem B 117:11326–11336

Snellenburg JJ, Laptenok SP, Seger R, Mullen KM, van Stokkum IHM (2012) Glotaran: a Java-based graphical user interface for the R package TIMP. J Stat Softw 49(3):1–22

Snellenburg JJ, Dekker JP, van Grondelle R, van Stokkum IHM (2013) Functional compartmental modeling of the photosystems in the thylakoid membrane at 77 K. J Phys Chem B 117(38):11363–11371

Veerman J, Vasilev S, Paton GT, Ramanauskas J, Bruce D (2007) Photoprotection in the lichen *Parmelia sulcata*: the origins of desiccation-induced fluorescence quenching. Plant Physiol 145:997–1005

Yamakawa H, Itoh S (2013) Dissipation of excess excitation energy by drought-induced nonphotochemical quenching in two species of drought tolerant moss: desiccation-induced acceleration of photosystem II fluorescence decay. Biochemistry 52:4451–4459

Yamakawa H, Fukushima Y, Itoh S, Heber U (2012) Three different mechanisms of energy dissipation of a desiccation-tolerant moss serve one common purpose: to protect reaction centres against photo-oxidation. J Exp Bot 63:3765–3776

Yamamoto HY, Kamite L (1972) The effect of dithiothreitol on violaxanthin de-epoxidation and absorbance changes in the 500 nm region. Biochem Biophys Acta 267:538–543